„BABEŞ-BOLYAI" UNIVERSITY
PHYSICS FACULTY
CLUJ-NAPOCA

Maria Maier

STRUCTURAL CHARACTERIZATION OF LaB_5AlGaO_{12} OXIDE COMPOUNDS

PHD THESIS SUMMARY

Scientific Supervisor:

Prof.dr. Simion Simon

Cluj-Napoca, 2016

„BABEŞ-BOLYAI" UNIVERSITY
PHYSICS FACULTY
CLUJ-NAPOCA

Maria Maier

STRUCTURAL CHARACTERIZATION OF LaB_5AlGaO_{12} OXIDE COMPOUNDS

PHD THESIS SUMMARY

Scientific Supervisor:

Prof.dr. Simion Simon

Cluj-Napoca, 2016

Content

Keywords:

xerogels; local structure; thermal stability; XRD; FTIR, borates; gallium; nuclear magnetic resonance

Introduction

The mixed porous oxides are intensely investigated in view of their potential applications as support materials for catalysis [1–3]. Lanthanum- and gallium-aluminoborate systems attracted special interest first for optical applications and then, by tailoring their structure, they were also considered for potential applications as support materials for catalysis. [4–8]. The presence of rare earths in these materials induces beside catalytic properties interesting magnetic properties [9]. It was shown that rare earths, like lanthanum, contribute to a reasonable preservation of sample porosity under thermal treatments [10] and along with post-transitional elements, like aluminium and gallium, and metalloid boron induce to their systems interesting optical, magnetic and catalytic properties.

All these properties strongly depend on materials structure. At the same time it is was shown that the borate glass systems containing aluminium and gallium prove a more stable glass network on account of AlO_4 and GaO_4 structural units which may cross-link the neighbouring borate chains [11]. It is expected that both in amorphous and crystalline porous materials, the presence of unusual coordinated cations, like penta-coordinated aluminium or/and gallium, would lead to more catalytically active sites. Systems with catalytic properties and structural stable at 850^oC are expected to display high stability and durability under practical working conditions for automotive catalysts, since the temperature of the exhaust gases in auto engines does not exceed this temperature [12,

13]. For specific applications, such as automotive catalytic converter, it is important to keep high porosity and specific surface area even at high temperatures, above 800°C. The stabilizing effect of rare earths, especially of lanthanum on γ-alumina is known [14], but the mechanism by which rare earth moves transition from γ- to α- Al_2O_3 toward higher temperatures is still under discussion.

This study is focused on the evolution of structural changes induced by increasing treatment temperature and due to 850^{o}C isothermal treatment applied for different times on amorphous and crystallized sol-gel–derived $La_2O_3{\cdot}Al_2O_3{\cdot}Ga_2O_3{\cdot}5B_2O_3$ system. The structure of samples heated for 30 min up to 900°C and the effect of 850^{o}C heat treatment time was investigated by differential thermal analysis (DTA), X-ray diffraction (XRD), Fourier transform infrared (FTIR) spectroscopy, Scanning electron microscopy (SEM) and magic-angle spinning nuclear magnetic resonance (MAS-NMR) analysis of ^{27}Al, ^{11}B, and ^{71}Ga nuclei.

Sample preparation and measurements were performed at the Institute for Interdisciplinary Research in Bio-Nano-Science and at the National Centre of Magnetic Resonance from the Faculty of Physics of the "Babes-Bolyai" University, Cluj-Napoca.

Synthesis

The sol-gel–derived LaB_5AlGaO_{12} system was prepared from aqueous solutions of $La(NO_3)_3{*}6H_2O$, $Al(NO_3)_3{*}9H_2O$, $Ga(NO_3)_3{*}xH_2O$, and H_3BO_3 of analytical purity grade, by thermal decomposition of starting nitrates and boric acid sustained by

simultaneous oxidation of glycerol (10 wt%). The mixture solved in desalinized water appears as a transparent solution at room temperature. A viscous gel is obtained after 2 h heating at 95°C. The further heating at this temperature leads to a spongious solid sample. Xerogel samples were obtained by heating for 30 min at different treatment temperatures, Tt, between 250°C and 950°C [15]. After thermal treatment, the samples were removed from the furnace and cooled down to room temperature.

A second set of $La_2O_3 \cdot Al_2O_3 \cdot Ga_2O_3 \cdot 5B_2O_3$ samples was prepared following sol–gel route using aqueous solutions of $La(NO_3)_3*6H_2O$, $Al(NO_3)_3*9H_2O$, $Ga(NO_3)_3*xH_2O$, and H_3BO_3, which were mixed together at room temperature and thereafter heated at 95^oC for 90 min, resulting in a viscous gel. Further heating at higher temperatures led to xerogel samples that remain amorphous up to 850^oC. The amorphous xerogel was isothermally treated at 850^oC for 0.5, 5, 15, 30 min, and 24 h [16].

The treatment temperatures were chosen based on the thermal analysis and X-ray diffraction results.

Experimental Procedure

The differential thermal analysis (DTA) and thermogravimetric analysis (TGA) runs were recorded with DTG-60H Shimadzu (Shimadzu Corporation, Kyoto, Japan) derivatograph at a heating rate of 10°C/min from room temperature to 1000°C. Alumina open crucibles and α-alumina powder as reference material

were used, and the measurement was made in flowing atmosphere of nitrogen/air at a flow rate of 70 mL/min.

X-ray diffraction (XRD) analyses were made on a Shimadzu XRD-6000 diffractometer using Ni-filtered CuK α radiation (λ =1.5418 Å) at a scanning speed of 2°/min.

The chemical analysis of the crystalline phase identified by XRD was carried out by energy-dispersive X-ray (EDX) spectroscopy with a FEI Quanta 3D FEG dual-beam scanning electron microscope using EDAX Genesis FEI software package for SEM–EDX system.

Fourier transform infrared (FTIR) spectra were recorded in reflection configuration in the range 4000–400 cm^{-1} with spectral resolution of 4 cm^{-1} using a Jasco FT-IR-6000 spectrometer (JASCO Corporation, Tokyo, Japan) and KBr pellet technique.

Magic-angle spinning nuclear magnetic resonance (MASNMR) spectra were recorded at room temperature for the ^{11}B, ^{27}Al, and ^{71}Ga nuclei in glass and glass–ceramic powdered samples spun at the magic angle 54.74° with a frequency of 20, 30, and 40 kHz, respectively, using a Bruker AVANCE 600 MAS-NMR (Karlsruhe, Germany). The deconvolution of spectra was performed by using Dmfit program [17].

Results and Discussion

The thermal analysis traces (Fig. 1) recorded after drying at 95°C of sol-gel–derived sample evidence several events. First weight losses observed in TG curve around 100°C are due to the loss of free

water and physically adsorbed water, accompanied by endothermic peaks in DTA trace.

The weight loss between 150°C and 300°C corresponds to removal of water and glycerol entrapped in the pores, and to decomposition of glycerol and residual nitrates, accompanied by exothermic peaks in DTA. The last weight loss is due to glycerol pyrolysis and to dehydroxylation process [18]. The exothermic events at higher temperatures denote the development of crystalline phases. The endothermic peak at 865°Cis associated with a melting process.

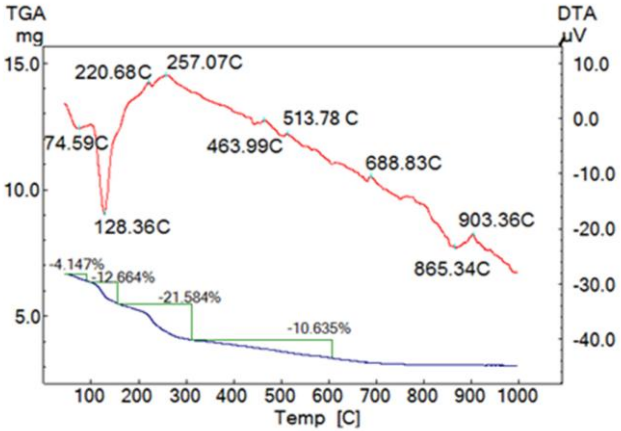

Fig. 1 *DTA and TGA curves recorded from the 95 °C dried sample*

For the first set of samples stands out that after 250°C treatment, the XRD pattern (Fig. 2) points out a weak diffraction line assignable to a small amount of residual nitrates used as precursors in sol-gel synthesis, which is less observed after 350°C treatment. Otherwise,

the DTA/TG data support the nitrates presence and decomposition up to 300°C. A large diffraction line typical for vitreous structure is observed after 700°C treatment (Fig. 2) and even after 800°C treatment (Fig. 3). Starting with 850°C heat treatment, the development of $LaAl_{2.03}(B_4O_{10})O_{0.54}$-type crystalline phase (JCPDS card no. 87-0484), of $La(Al,Ga)_{2.03}B_4O_{10.54}$ composition, is evidenced (Fig. 3).

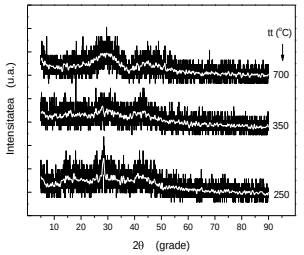

Fig. 2 *X-ray diffraction patterns of the samples heat treated at 700 °C for 30 min.*

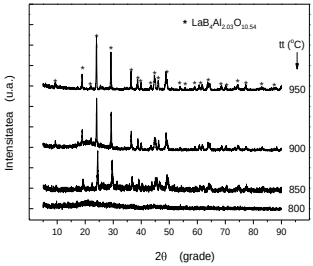

Fig.3 *X-ray diffraction patterns of the samples heat treated at 900 °C for 30 min*

The X-ray diffraction analysis for the second set, points out the vitreous state of $LaAlGaB_5O_{24}$ xerogel, that is still preserved after 0.5 and 5 min treatment at 850°C (Fig.4). After 15 min treatment, nanocryatallites of $LaAl_{2.03}(B_4O_{10})O_{0.54}$ type [19] are developed. The chemical composition of $La(Al,Ga)_{2.03}B_4O_{10.54}$ crystalline phase, determined by EDX analysis, points out that about a third of aluminium sites are occupied by gallium. The average crystallite size was estimated using the Scherrer formula; the values

increase with treatment temperature from 27 to 37 nm, typical for nanostructured materials. The large diffraction line around 2h= 21° recorded after 900°C treatment indicates the presence of a boron-rich glassy phase related to the melting event evidenced in DTA curve at 865°C (Fig. 1). In $LaAl_{2.03}(B_4O_{10})O_{0.54}$ crystalline phase boron and aluminium are only tetracoordinated and pentacoordinated, respectively. The treatment extension up to 24 h enhances the growth of this crystalline phase, without to promote the development of any other structurally ordered phases. The crystallites size, estimated with Scherrer equation, slightly increases from 25 nm after 15 min, to 27 nm after 30 min, and to 31 nm after 24 h treatment at 850^{o}C. It is worth to note the very weak size increase from the value determined after 15 min treatment to that reached after the much longer 24 h treatment, suggests that the number of crystallites increased and not so much their size.

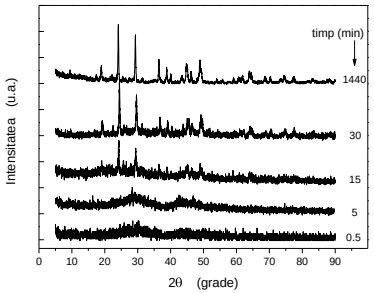

Fig. 4 *XRD patterns after different treatment times at 850 ^{o}C*

In the $LaAl_{2.03}(B_4O_{10})O_{0.54}$ lanthanum–aluminium borate phase, each La ion is coordinated by six O atoms to form a trigonal

prism, each Al is coordinated by five O atoms to form a pyramid, whereas B ion is coordinated by four O atoms in a tetrahedral arrangement, [19] as it was confirmed for aluminium and boron by MAS-NMR measurements [20]. Minor contributions from $LaBO_3$ and $La(BO_2)_3$, or from $GaBO_3$ crystalline phases of lanthanum, gallium, or aluminium borates are not excluded, but even if they would be formed in samples treated at high temperature they are overwhelmed by $LaAl_{2.03}(B_4O_{10})O_{0.54}$ crystalline phase.

Elemental analysis of the crystalline phase identified by X-ray diffraction was carried out with a FEI Quanta 3D EGF scanning electron microscope using EDAX Genesis FEI processing program for SEM-EDX system. The chemical composition of the $La(Al,Ga)_{2.03}B_4O_{10.54}$ crystalline phase determined by spectroscopic analysis of energy dispersive X-ray (EDX) on scanning electron microscopy (scanning electron microscope / SEM) shows by the Ga / Al = 0.3 ratio that approximately one third of the positions are occupied by gallium aluminium (Fig. 5 and 6). Elemental analysis was performed by EDAX ZAF quantitation.

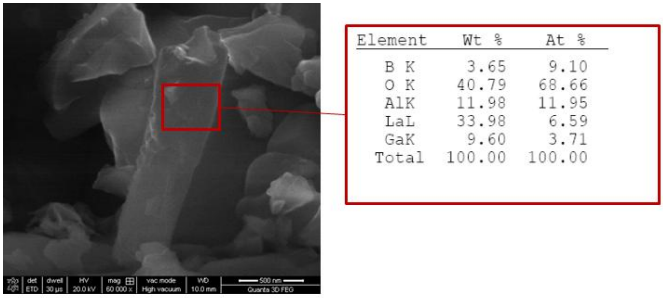

Fig. 5 *SEM and EDX results for the sample heat treated for 30 minutes at 900 ^oC*

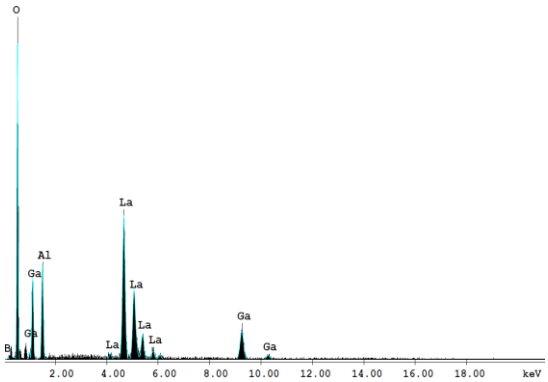

Fig. 6 *EDX spectrum of the sample heat treated for 30 minutes at 900 ^{o}C.*

More information on structural changes caused by thermal treatment can be obtained using infrared spectroscopy. The differences observed in the absorption bands recorded in the spectral range up to 2000 cm^{-1} (Fig. 7) are due to the effect of treatment temperature on the structural units. Crystalline and non-crystalline borates consist of different structural arrangements, which are composed of BO_3^{-3} triangles and BO^{-4} tetrahedra that are giving in infrared spectra–specific lines around 1300–1500 cm^{-1} and 850–1050 cm^{-1}, respectively [21– 25] One remarks an apparent resemblance for the spectra recorded from samples heat treated up to 700°C and for the spectra recorded from samples heat treated above 800°C. The band at 1645 cm^{-1} corresponds to bending vibration of water (H–O–H bending). The sharp band at 1384 cm^{-1} assigned to residual nitrate groups disappears by further thermal treatment. The large dominant band around 1464 cm^{-1} is assigned to BO_3 units, the 1194 cm^{-1} band to B–O stretching vibrations of BO_3 units, that at 770 cm^{-1} is related

to Al–O stretching vibrations of tetrahedral AlO_4 groups, and the bands in 650–400 cm^{-1} region are associated with stretching modes of AlO_6 octahedra, but for 646 cm^{-1} band could be also considered B–O out-of-plane bending vibrations of BO_3 units as well as vibrations of La–O or Ga–O bonds in lanthanum or gallium polyhedra [26–28]. The local structure from amorphous xerogel changes by increasing the heat treatment temperature. New bands around 1050, 960, and 857 cm^{-1} are assigned to BO_4 tetrahedra, and that at 714 cm^{-1} mainly to the penta-coordinated aluminium s [29]. The peak around 857 cm^{-1} could incorporate aluminium. Because in the $LaAl_{2.03}B_4O_{10.5}$ phase aluminium is only penta-coordinated, the AlO_4 and AlO_6 species would be excluded, or could be considered only related to other minor phases which did not impose in XRD patterns.

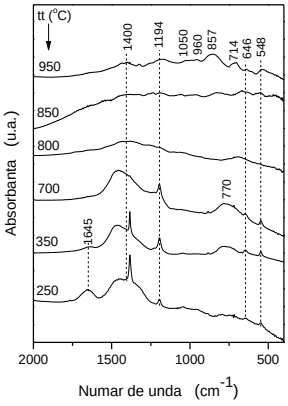

Fig. 7 *FTIR spectra of samples obtained after increasing treatment temperatures.*

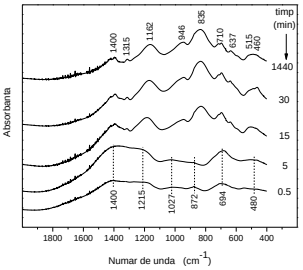

Fig. 8 *FTIR spectra after different treatment times at 850 ^0C.*

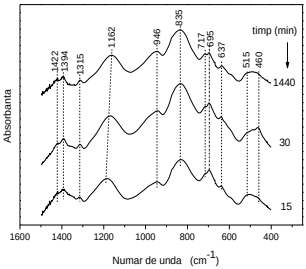

Fig. 9 *FTIR spectra of samples treated from 15 min up to 24h at 850 ^{o}*

In multicomponent borate systems the amorphous matrix mainly consists of BO_3 and BO_4 units [23]. In the infrared spectra of still vitreous samples after 0.5 and 5 min treatment, the absorption bands occur around 480, 694, 872, 1027, 1215 and 1400 cm^{-1} (Fig. 8). The 1215 and 1400 cm^{-1} bands are assigned to BO_3 units, that at 872 and 1027 cm^{-1} to BO_4 units, while 480 and 694 cm^{-1} bands are related to hexacoordinated and pentacoordinated aluminium , respectively [30]. A contribution from tetracoordinated aluminium to the large band around 694 cm^{-1} should be also considered [31].

In Ga_2O_3 mixed glasses was identified an absorption band around 610–620cm^{-1} assigned to the vibrations of GaO_4 structural units [11, 32]. Ga_2O_3 is considered to act as a network former if Ga^{3+} ions take preferentially four-fold coordination in oxide glasses. The excess negative charge on GaO_4 tetrahedra are compensated either by localization of a modifier ion nearby or by generation of three-fold oxygens. The GaO_4 tetrahedrons may enter the glass network and alternate with BO_4 tetrahedrons. In some glass networks, the

gallium ions are also found to be in modifier position with GaO_6 structural units [11, 33]. Gallium is heavier than aluminium and Ga^{3+} has lower field strength than Al^{3+}; therefore is expected a shift of the infrared absorption band to lower wavenumbers than for aluminium. After 15 min treatment, and up to 24 h treatment, the infrared spectra are highly similar (Fig. 9) but different from that recorded from amorphous samples. The former large band around 1400 cm^{-1} appears with three components at 1422, 1394 and 1315 cm^{-1}, all assigned to different stretching vibrations of B–O bonds in BO_3 units modified by local distortions [30, 34, 35]. These components are clearly evidenced in the smoothed absorption lines (Fig. 10). The deconvolution with three lines does not fit well the large band, but roughly comparing the relative intensity of 1422, 1394 and 1315 cm^{-1} components one can estimate their contribution as function of treatment time. One remarks the increase of 1315 cm^{-1} component on account of 1422 and1394 cm^{-1} components (Table 1). The higher vibration frequency of the B–O bonds which give rise to 1315 cm^{-1} component indicates a shortening of the corresponding B–O bond lengths. The absorption band occurred at 1215 cm^{-1} in the vitreous samples, also assigned to BO_3 units, is shifted to lower wavenumbers after crystallization, with a light dependence on treatment time, namely to 1188 cm^{-1} after 15 min treatment and to 1162 cm^{-1} after 24 h treatment. The new band recorded at 946 cm^{-1}, as well as the band at 835 cm^{-1}, that occurs shifted to lower wavenumbers as compared with 872 form the vitreous samples, are assigned to BO_4 units. The analysis of the bands related to BO_3 and BO_4 units shows the

considerable increase of tetrahedral BO_4 units after 15 min treatment. The bands around 710 cm^{-1} (Fig. 8) correspond to that recorded around 694 cm^{-1} for non-crystalline xerogels, assigned to tetra- and pentacoordinated aluminium , and after treatments longer than 15 min two components at 695 and 717 cm^{-1} are evidenced (Fig. 9), which denotes two different surroundings of aluminium units in the crystallized samples. The decomposition with two lines fits well the absorption in this range (Fig. 11) and points out the preponderance of 717 cm^{-1} line as treatment time increases to 24 h (Table 2).

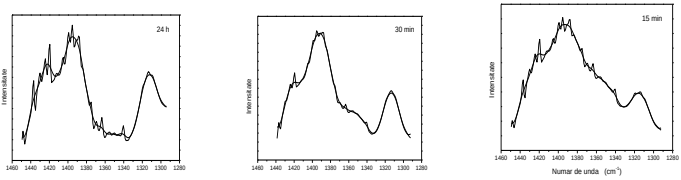

Fig. 10 *Smoothed FTIR lines in 1290-1450 cm^{-1} spectral range.*

Tabelul 1 *Treatment time dependence of the relative contributions (%) to 1422, 1394 and 1315 cm^{-1} components.*

Componenta		**1422 cm^{-1}**	**1394 cm^{-1}**	**1315 cm^{-1}**
Timpul de tratament	**15 min**	34	50	16
	30 min	26	52	22
	24 h	30	43	27

In infrared spectra of inorganic aluminates [36], the characteristic frequency ranges are „condensed" AlO_4 tetrahedra in the 900–700 cm^{-1}, „isolated" AlO_4 tetrahedra 800–650cm^{-1}, „condensed" AlO_6 octahedra in the 680–500 cm^{-1} and isolated" AlO_6 octahedra in the 530–400 cm^{-1}. Considering the component at 695

cm^{-1} arising from "isolated" AlO_4 units, one remarks with increasing treatment time the increase of the component assigned to AlO_5 units. Nevertheless, for the bands at 637, 515 and 460 cm^{-1} associated with vibrations of AlO_6 octahedra [31] one remarks an increased intensity. With regard to 637 cm^{-1} band, vibrations of La–O or Ga–O bonds in lanthanum or gallium polyhedra are not excluded [30,26–28], and for 515 and 460 cm^{-1} bands should be also considered vibrations like that observed for Ga_2O_3 [37], La_2O_3 [38],or vibrations arising from bonds between cations via oxygen.

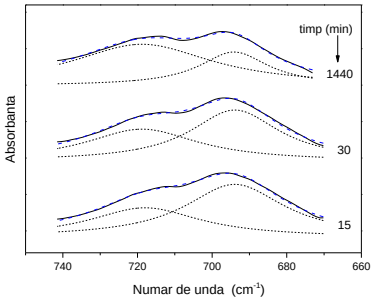

Fig. 11 *Line deconvolution in 670-740 cm^{-1}spectral range.*

Tabelul 2 *Treatment time dependence of the relative contributions (%) to 717 and 695 cm^{-1} components.*

Componenta		**717 cm^{-1}**	**695 cm^{-1}**
Timpul de tratament	**15 min**	38.5	61.5
	30 min	44.3	55.7
	24 h	73.3	26.7

All these structural similarities preserved after development of $LaAl_{2.03}(B_4O_{10})O_{0.54}$ type crystalline phase at 850°C, regardless of treatment time, support that the investigated system is thermally stabile at high temperatures, which is a desirable property for a prospective catalyst material working in a close temperature range.

The analysis of ^{27}Al MAS-NMR spectra (Fig. 12) clearly supports the disappearance of aluminium tetra- and hexacoordinated species after 900°C heat treatment (Table 3). The contribution of different species [39] was determined based on spectra deconvolution, as illustrated for 800°C treated sample (Fig. 13).

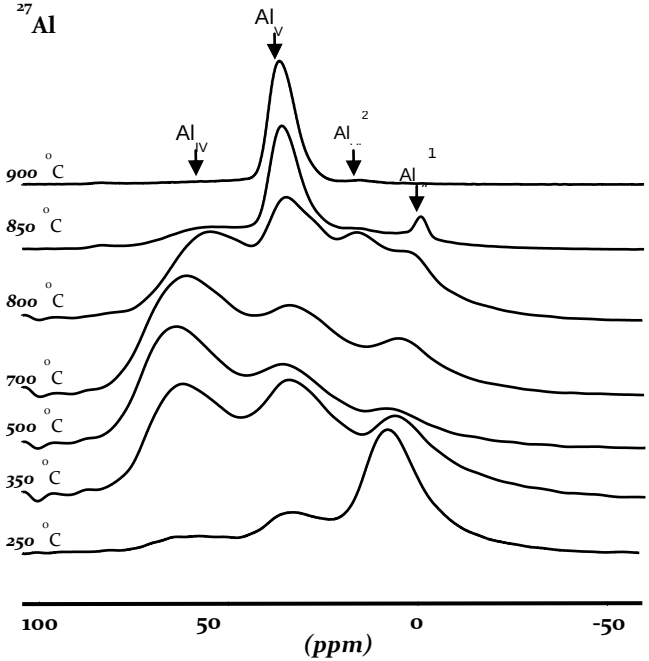

Fig. 12 *^{27}Al MAS NMR spectra after heat treatment at different temperatures.*

The errors are estimated to ~0.5 ppm for the isotropic chemical shift (diso) and ~2.5% for the fraction of different species expressed by the relative intensity (I) of deconvoluted lines. The high content of penta-coordinated aluminium after 900°C treatment is desirable for catalytic applications [40 – 42].

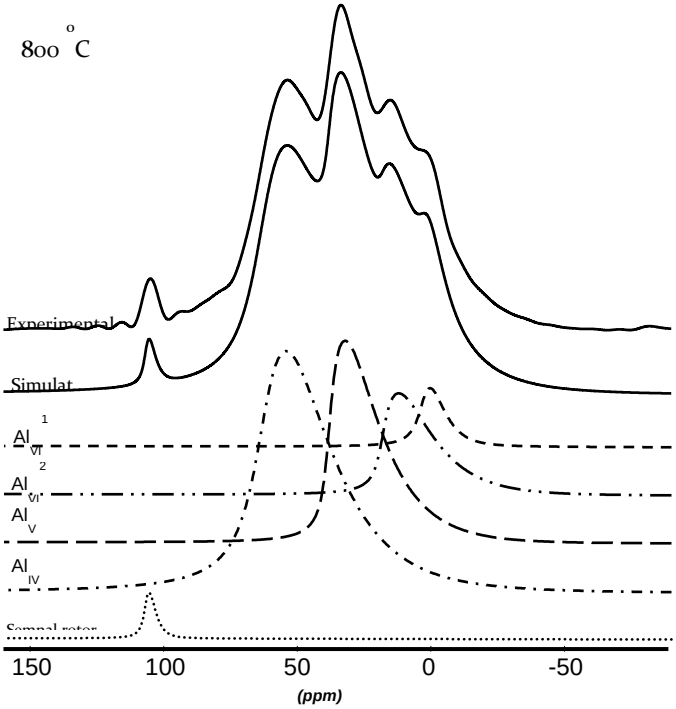

Fig. 13 *Deconvolution of ^{27}Al MAS NMR spectrum with Dmfit program for the sample obtained after 800°C heat treatment.*

Tabelul 3 *The Isotropic Chemical Shift (δ_{iso}) and Fraction of Aluminum Species Expressed by the Relative Intensity (I) of Deconvoluted ^{27}Al MAS-NMR Lines.*

tt(°C)	**250**		**350**		**500**		**700**		**800**		**850**		**900**	
Unitati	**δ_{iso} (ppm)**	**I (%)**	**δ_{iso} (ppm)**	**I (%)**	**δ_{iso} (ppm)**	**I (%)**	**δ_{iso} (ppm)**	**I (%)**	**δ_{iso} (ppm)**	**I (%)**	**δ_{iso} (ppm)**	**I (%)**	**δ_{iso} (ppm)**	**I (%)**
Al_{IV}	6,	13.8	61.5	49.7	63.0	67.6	57.6	58.5	54.5	45.0	82.5 55.7	22.8 0.4	80.2 61.8	1.5 0.3
Al_V	32.5	17.0	31.8	33.6	32.2	25.0	32.4	27.7	32.4	30.6	35.2	56.1	35.6	96.9
Al_{VI}	6.5	69.2	5.3	16.7	5.1	7.4	8.2	13.8	12.8 0.5	14.7 9.7	12.9 -1.4	15.8 4.9	12.8	1.3

Based on deconvolution of ^{11}B MAS-NMR spectra (Figs. 14 and 15), the contributions of BO_3 and BO_4 units were estimated. Two chemical shifts are evidenced for BO_3 units, denoting their occurrence in two environments. The increase in treatment temperature favours the development of BO_4 units (Fig. 14). The large amount of B_{IV}, 72.1%, estimated from ^{11}B MAS-NMR measurements after 900°C treatment (Table 4), supports the assignment of the 857 cm^{-1} band from FTIR spectrum (Fig. 7) to tetra-coordinated boron without contribution from tetra-coordinated aluminium, in full agreement also with ^{27}Al MAS-NMR results (Table 3).

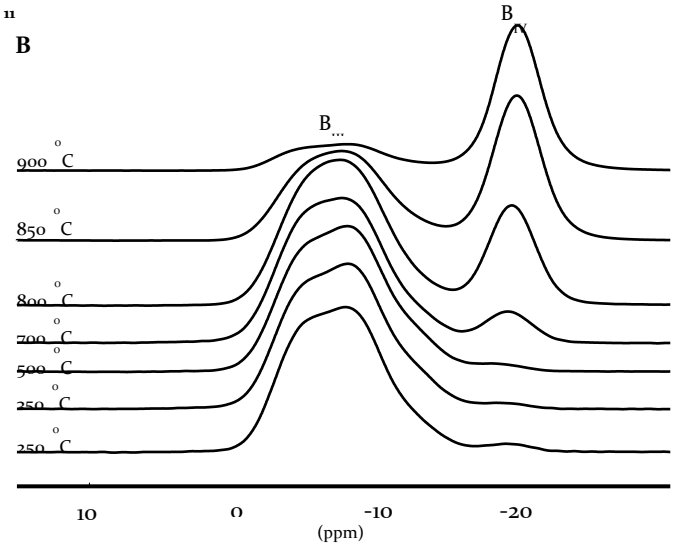

Fig. 14 *^{11}B MAS-NMR spectra after treatments at different temperatures*

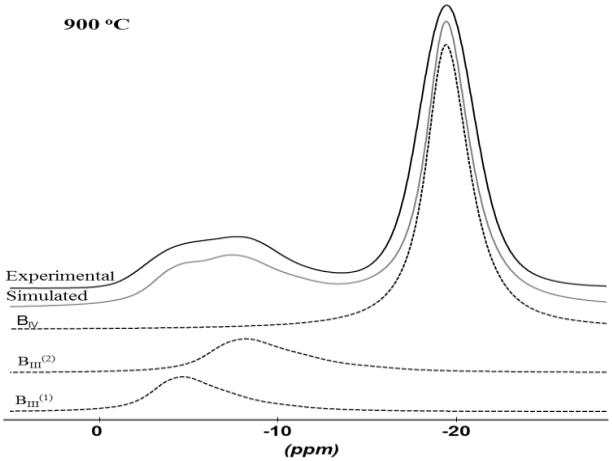

Fig. 15 *Deconvolution of ^{11}B MAS NMR spectrum with Dmfit program for the sample obtained after 900°C heat treatment.*

By knowing that in $LaAl_{2.03}(B_4O_{10})O_{0.54}$ crystalline phase only tetra-coordinated boron is present, we can assign the three coordinated species to boron-rich glassy phase that separate/segregate due to the higher boron content in starting composition (B5) compared with the boron content in the developed crystalline phase (B4). From our experience, [20, 23, 40] to develop a rich boron crystalline phase at relative high temperatures an excess of boron is needed.

Tabelul 4 *The Isotropic Chemical Shift (δ_{iso}) and Fraction of Boron Species Expressed by the Relative Intensity (I) of Deconvoluted ^{11}B MAS-NMR Lines.*

tt (°C)	**250**		**350**		**500**		**700**		**800**		**850**		**900**	
Unitati	**δ_{iso} (ppm)**	**I (%)**	**δ_{iso} (ppm)**	**I (%)**	**δ_{iso} (ppm)**	**I (%)**	**δ_{iso} (ppm)**	**I (%)**	**δ_{iso} (ppm)**	**I (%)**	**δ_{iso} (ppm)**	**I (%)**	**δ_{iso} (ppm)**	**I (%)**
B_{III}	-4.3 -8.4	23.9 72.8	-4.90 -8.4	21.6 76.5	-4.5 -8.5	18.2 78.6	-4.7 -8.3	24.8 65.6	-4.75 -8.21	14.1 60.1	-4.6 -8.4	10.0 44.4	-4.5 -8.2	3.8 24.1
B_{IV}	-9.0	3.3	-18.9	1.9	-18.3	3.2	-19.0	9.5	-19.5	25.8	-19.7	45.6	-19.9	72.1

On the other hand, the analysis of ^{71}Ga NMR spectra (Fig. 16) based on their deconvolution (Fig. 17) evidence that after 250°C treatment only hexa-coordinated gallium occurs. After treatments between 350°C and 800°C, beside Ga_{VI}, both Ga_{IV} and Ga_V were identified. The penta-coordination of gallium in oxide glasses and ceramics was reported in few studies, [43 –48] but only one gallium compound with exclusively penta-coordinated gallium was mentioned [44].

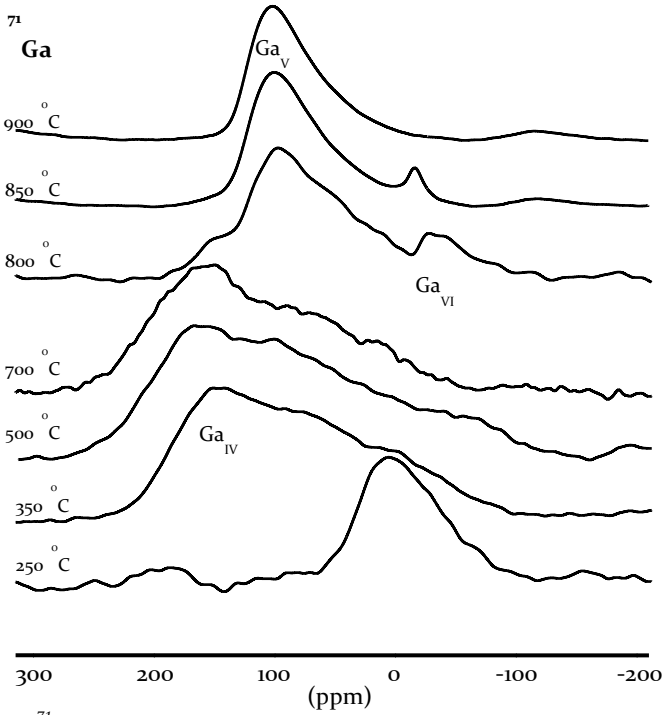

Fig. 2 *^{71}Ga MAS NMR spectra of samples treated at different temperatures.*

Our current investigation points out that the heat-treatment temperature enhancement to 850°C already leads to 95.3% Ga_V, and after 900°C treatment exclusively penta-coordinated gallium is evidenced (Table 5).

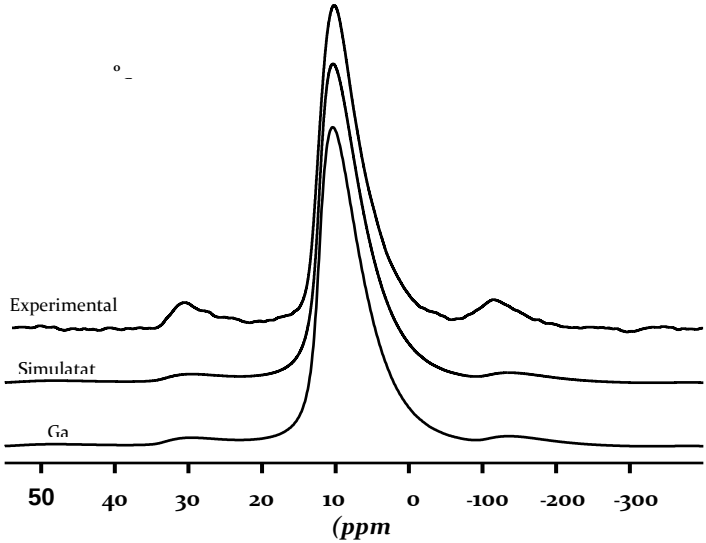

Fig. 3 *Deconvolution of ^{71}Ga MAS NMR spectrum with Dmfit program for the sample obtained after 900°C heat treatment.*

These data corroborated with earlier results, [26] which reported that in $25La_2O_3$ •xGa_2O_3•(75-x) B_2O_3 and $25La_2O_3$ •xAl_2O_3•(75-x)B_2O_3 ($0 \leq x \leq 25$ mol%) glass systems Al_2O_3, Ga_2O_3, and B_2O_3 act as glass formers, whereas La_2O_3 acts as network modifiers that open a new insight regarding the investigated $La_2O_3 \cdot Al_2O_3 \cdot Ga_2O_3 \cdot 5B_2O_3$ system, wherein starting with 850°C treatment the crystalline phase of $LaAl_{2.03}(B_4O_{10})O_{0.54}$ type is developed. In this phase, gallium is replacing partially aluminium. The assumption is further supported by properties resemblance between gallium and aluminium compared against that of boron and lanthanum (Table 6). The analysis of ^{11}B, ^{27}Al, and ^{71}Ga MAS-NMR

results for treatments above 850°C (Figs. 18-23) indicates for gallium coordination similarities only with aluminium, and after 900°C both appear only pentacoordinated. We consider that the crystalline phase identified as $LaAl_{2.03}(B_4O_{10})O_{0.54}$ for the actual $La_2O_3{\cdot}Al_2O_3{\cdot}Ga_2O_3{\cdot}\ 5B_2O_3$ investigated system is $La(Al/Ga)_{2.03}(B_4O_{10})O_{0.54}$.

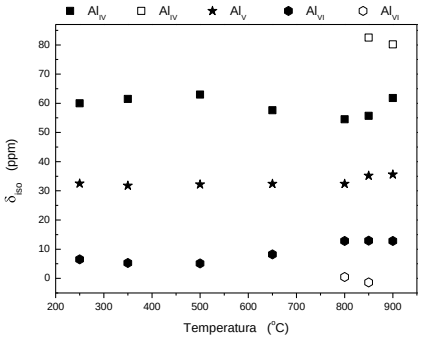

Fig. 18 *The Isotropic Chemical Shift (δ_{iso}) dependence of Al_{IV} (■, □) tetra-, Al_V (*) penta-, and Al_{VI}(●, ○) hexa-coordinated aluminum species on treatment temperature.*

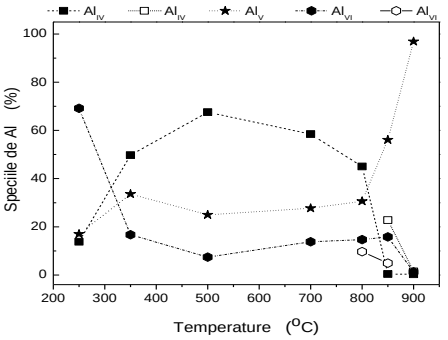

Fig. 19 *Dependence of Al_{IV} (■, □) tetra-, Al_V (*) penta-, and Al_{VI} (●, ○) hexa-coordinated aluminum species on treatment temperature. The lines are only guide to the eye.*

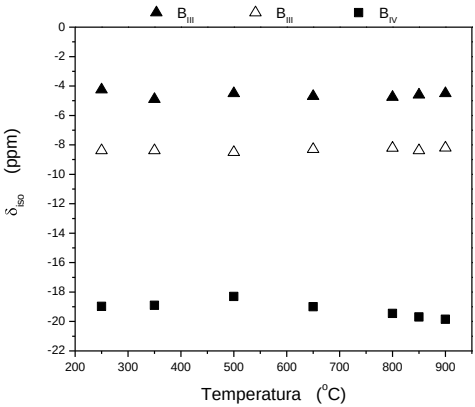

Fig. 20 *The Isotropic Chemical Shift (δ_{iso}) dependence of B_{III} (N, M) tri- and B_{IV} (■) tetracoordinated Boron species on treatment temperature.*

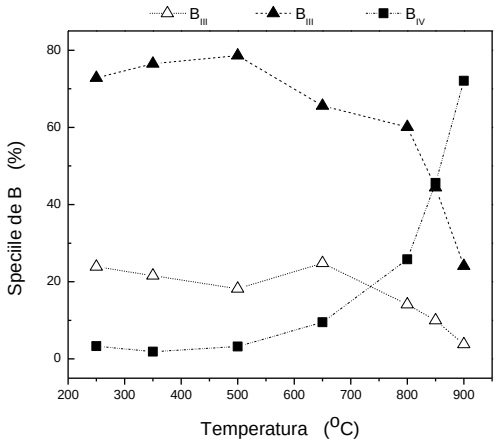

Fig. 21 *Dependence of B_{III} (N, M) tri- and B_{IV} (■) tetracoordinated boron species on treatment temperature. The lines are only guide to the eye.*

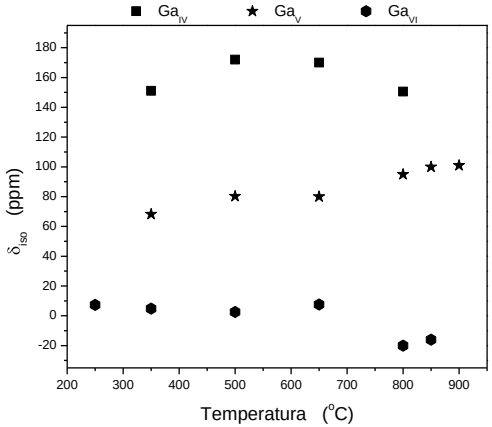

Fig. 22 *The Isotropic Chemical Shift (δ_{iso}) dependence of Ga_{IV} (■) four-, Ga_V (*) penta-, and Ga_{VI} (●) hexa-coordinated gallium species on treatment temperature..*

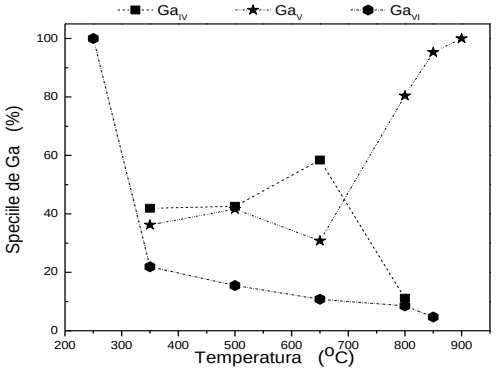

Fig. 23 *Dependence of Ga_{IV} (■) four-, Ga_V (*) penta-, and Ga_{VI} (●) hexa-coordinated gallium species on treatment temperature. The lines are only guide to the eye .*

Tabelul 5 *The Isotropic Chemical Shift (δ_{iso}) and Fraction of Gallium Species Expressed by the Relative Intensity (I) of Deconvoluted ^{71}Ga MAS-NMR Lines.*

tt(°C)	250		350		500		700		800		850		900	
Unitati	**δ_{iso}(ppm)**	**I(%)**	**δ_{iso}(ppm)**	**I(%)**	**δ_{iso}(ppm)**	**I(%)**	**δ_{iso}(ppm)**	**I(%)**	**δ_{iso}(ppm)**	**I(%)**	**δ_{iso}(ppm)**	**I(%)**	**δ_{iso}(ppm)**	**I(%)**
Ga_{IV}			151.0	41.9	172	42.6	170	58.4	150.5	11.1				
Ga_{V}			68.2	36.2	80.2	41.6	80	30.8	95	80.4	100	95.3	101	100
Ga_{VI}	7.3	100	4.8	21.9	2.5	15.5	7.5	10.8	-20	8.5	-16	4.7		

MAS-NMR studies on ^{27}Al, ^{11}B and ^{71}Ga nuclei from heat treated samples above 850^{o}C highlight the similarities concerning the gallium and aluminium coordination, pointing out that after a 900° C treatment gallium appears only pentacoordinated, like aluminium. Thus NMR results support the conclusion that $LaAl_{2.03}(B_4O_{10})O_{0.54}$ type crystalline phase identified for the $La_2O_3{\cdot}Al_2O_3{\cdot}Ga_2O_3{\cdot}5B_2O_3$ system composition investigated in this work is $La(Al/Ga)_{2.03}(B_4O_{10})O_{0.54}$.

All these data combined with the other results [49] obtained for the lantano-Gallo-borate $25La_2O_3{\cdot}xGa_2O_3{\cdot}(75\text{-}x)B_2O_3$ and $25La_2O_3{\cdot}xAl_2O_3{\cdot}(75\text{-}x)B_2O_3$ ($0 \leq x \leq 25$ mol%) systems showing that Al_2O_3, Ga_2O_3 and B_2O_3 acts as vitreous network formers, while

La_2O_3 act as network modifier, open a new perspective on the $La_2O_3 \cdot Al_2O_3 \cdot Ga_2O_3 \cdot 5B_2O_3$ investigated system, where following the thermic treatment, starting with 850°C is developing a single $LaAl_{2.03}(B_4O_{10})O_{0.54}$ crystalline phase type, in which aluminum atoms are partially replaced by gallium atoms. This is explained by the similarities between the properties presented by gallium and aluminum, different from those of lanthanum and boron (Table 6).

The small difference between the ionic radius of aluminum and gallium, their electronegativity and higher proximity strength of M-O connection, compared to the values for boron and lanthanum, may explain the partial replacement of aluminum and gallium in crystallites $La(Al/Ga)_{2.03}(B_4O_{10})O_{0.54}$ type $LaAl_{2.03}(B_4O_{10})O_{0.54}$.

Tabelul 6 *Ionic Radius, Coordination Type, Ionic Field Strength, Single-Bond Strength with Oxygen, and Electronegativity of the Cations Entering in the Investigated System.*

Caion/M	Coord.	Raza ionica Shannon [65, 66] (Å)	Intensitatea de camp ionic ($Å^{-2}$)	Intensitatea/ taria legaturii M-O [67] kJ/mol	Electroneg. Pauling
B^{3+}	4	0.25	48	808.8 ±20.9	2.04
Al^{3+}	4 6	0.53 0.675	10.68 6.58	511 ±3	1.61
Ga^{3+}	4 6	0.61 0.76	8.06 5.19	353.5 ±41.8	1.81

MAS NMR spectra analysis, on the ^{27}Al, ^{71}Ga and ^{11}B nuclei in heat treated samples at 850°C for 0.5 minutes to 24 hours

gives results in good agreement with the results obtained by FTIR spectroscopy and enhanced them.

^{27}Al nuclei (Fig. 24) in the heat treated sample for 24 hours appear only pentacoordinated aluminium species, as well as ^{71}Ga nuclei (Fig. 25). The data obtained for 24 hours annealed samples are in good correlation with those obtained for samples treated at 900°C for 30 min. We notice, however, a broadening of the line attributed gallium pentacoordinated in the sample obtained after 24 hours at 850°C treatment, which shows a higher sensitivity of this species to prolonged exposure to 850°C temperatures.

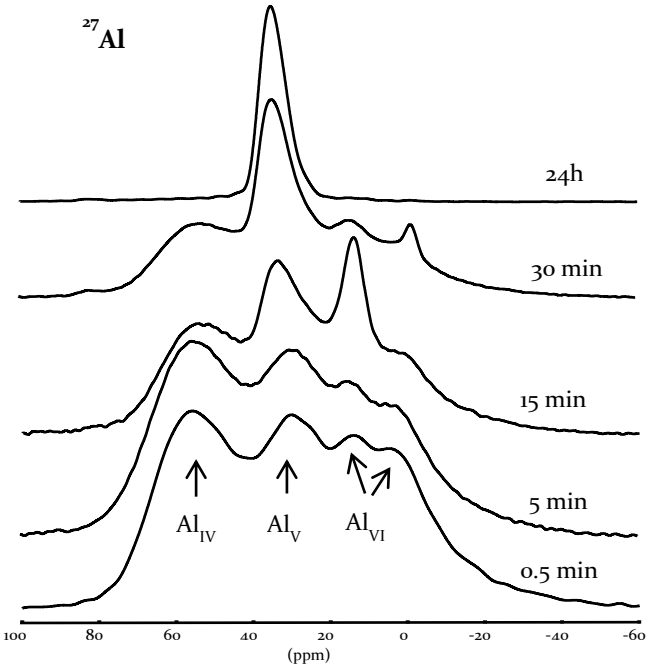

Fig. 24 *^{27}Al MAS-NMR spectra dependence on treatment duration applied on LaB_5AlGaO_{12} xerogel at 850 ^oC*

Results on ^{11}B nuclei (Fig. 26) confirm the overwhelming preponderance of BO_4 units to BO_3 units with increasing duration of heat treatment [50]. The increase in the number of BO_4 units after 15 minutes of treatment at 850^oC highlighted by analyzing infrared absorption bands is very well supported by the evolution of BO_3 and BO_4 units as shown by ^{11}B MAS-NMR.

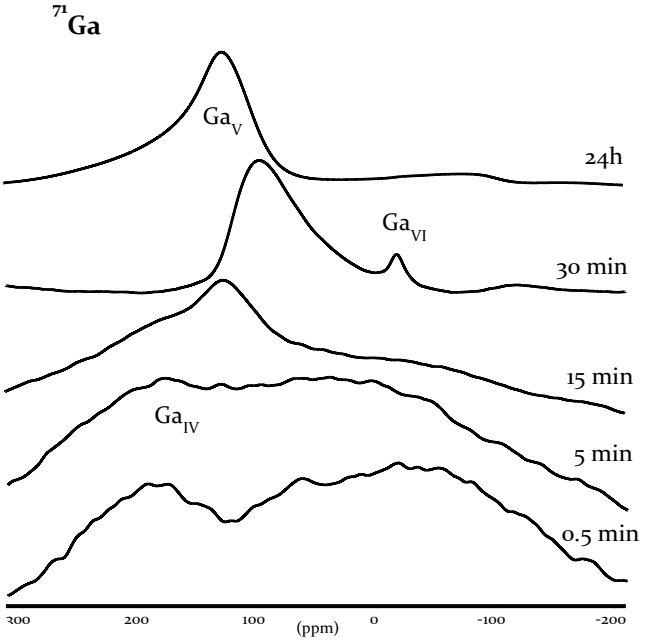

Fig. 25 *^{71}Ga MAS-NMR spectra dependence on treatment duration applied on LaB_5AlGaO_{12} xerogel at 850 ^oC*

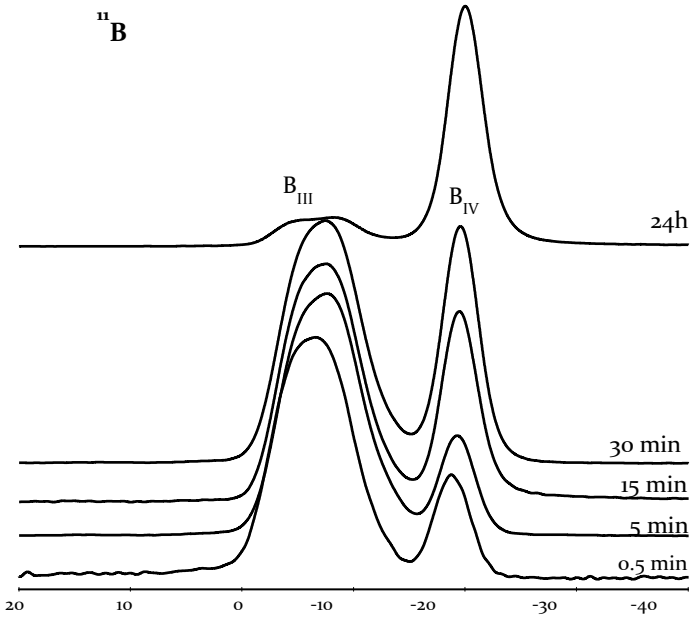

Fig. 26 *^{11}B MAS-NMR spectra dependence on treatment duration applied on LaB_5AlGaO_{12} xerogel at 850 ^oC*

Conclusions

A new compound with $La(Al/Ga)_{2.03}(B_4O_{10})O_{0.54}$ composition of similar structure with $LaAl2_{.03}(B_4O_{10})O_{0.54}$ crystalline phase, wherein aluminium and gallium are only penta-coordinated, was synthesized for the first time in sol-gel–derived $La_2O_3{\cdot}Al_2O_3{\cdot}Ga_2O_3{\cdot}5B_2O_3$ system heat treated at 850°C for 30 min. In $La(Al/Ga)_{2.03}(B_4O_{10})O_{0.54}$ crystalline compound, about a third of aluminium atoms are replaced by gallium atoms. With increasing heat-treatment temperature up to 800°C, during removal of water molecules, residual nitrates, and hydroxyl groups, the samples

structure is kept amorphous. Around 850°C, as result of crystallization, the fraction of different structural units, as identified by ^{11}B, ^{27}Al, and ^{71}Ga NMR analysis, is dramatically changed. These analyses proved that the penta-coordinated aluminium and gallium species are already consolidated in the noncrystalline precursors.

Sol–gel derived $LaAlGaB_5O_{12}$ system keeps the amorphous state after short treatment at 850^oC, for 0.5 and 5 min. After 15 min treatment, nanocrystallites of $LaAl_{2.03}(B_4O_{10})O_{0.54}$ type are developed and this crystalline phase is solely preserved by increasing the treatment time up to 24 h. FTIR results evidence that the local structure of amorphous samples consist of BO_3, BO_4, AlO_4, AlO_5 and AlO_6 polyhedra. In the crystallized samples a considerable increase of tetrahedral BO_4 units is observed, and for BO_3 species are identified three different vicinities. The increase of pentacoordinated aluminium species in these samples is desirable for catalytic applications. By increasing the treatment time at 850^oC from 15 min to 24 h, the structure of $LaAlGaB_5O_{12}$ system is very weakly affected, that recommend it once more for catalytic applications in this temperature range of interest for auto engines.

References

1. S. Jauhar, S. Singhal, Substituted cobalt nano-ferrites, CoMxFe2 - xO 4(M¼Cr 3 þ,Ni2 þ,Cu2 þ,Zn2 þ; 0.2rxr1.0) as heterogeneous catalysts for modified Fenton's reaction, Ceram. Int. 40 (2014) 11845–11855.

2. G. Frenzer, W.F. Maier, Amorphous porous mixed oxides: sol–gel ways to a highly versatile class of materials and catalysts, Annu. Rev. Mater. Res. 36 (2006) 281–331.

3. M. Vasilescu, G. Borodi, S. Simon, MAS NMR and SEM study of local structure changes induced by heat treatment in La2B4Al2O 12, J. Optoelectron. Adv. Mater. 5 (2003) 153–156 5.

4. R. K. Brow, D. R. Tallant, I. N. Chakraborty, and D. E. Day, "Effect of R3+ Ions on the Structure and Properties of Lanthanum Borate Glasses," J. Am. Ceram. Soc., 68 [12] 641–5 (1985).

5. G. L. Turner, "Polyhedral Arrangements in Lanthanum Aluminoborate Glasses," J. Am. Ceram. Soc., 80 [5] 1239–44 (1997).

6. Y. Shin, D. W. Lee, J. Hong, K. Kwak, and K. M. Ok, "Second-Harmonic Generating Properties of Polar Noncentrosymmetric Aluminoborate Solid Solutions, Al5-xGaxBO9 (0.0≤ x≤ 0.5)," Dalton T., 41 [11] 3233–8 (2012).

7. B. Ma, R. Cong, W. Gao, and T. Yang, "Photocatalytic Overall Water Splitting Over on Open-Framework Gallium Borate Loaded With Various Cocatalysts," Catal. Commun., 71,17–20 (2015).

8. T. Yang, A. Bartoszewicz, J. Ju, J. Sun, Z. Liu, et al., "Microporous Aluminoborates With Large Channels: Structural and

Catalytic Properties," Angew. Chem. Int. Edit., 50 [52] 12555–8 (2011).

9. O. K. Kuvandikov, N. I. Leonyuk, Kh. O. Shakarov, Z. M. Shodiev, B. U. Amonov, et al., "Magnetic Properties of Rare-Earth Ferro- and Aluminoborates RM3(BO3)4 (M= Fe or Al and R= Y, Gd, Er, or Dy)," Russ. Phys. J., 56 [12] 1398–402 (2014).

10. D. Neagu, J.T.S. Irvine, Structure and properties of La0.4Sr0.4TiO3 Ceramics for use as anode materials in solid oxide fuel cells, Chem. Mater. 22 (2010) 5042–5053.

11. M. Srinivasa Reddy, G. Naga Raju, G. Nagarjuna, and N. Veeraiah, "Structural Influence of Aluminium , Gallium and Indium Metal Oxides by Means of Dielectric and Spectroscopic Properties of CaO–Sb2O3–B2O3 Glass System," J. Alloy. Compd., 438 [12] 41–51 (2007).

12. W.Z. Zhao, T. Suna, K.T.V. Grattana, Y.H. Shen, A.I. Al-Shamma'a, Temperature monitoring of vehicle engine exhaust gases under vibration condition using opticalfibre temperature sensor systems, J. Phys. Conf. Ser. 45 (2006) 215–222.

13. S. Sun, W. Chu, W. Yang, Ce–Al mixed oxide with high thermal stability for Diesel soot combustion, Chin. J. Catal. 30 (2009) 685–689.

14. D.L. Trimm, Catalyst design for reduced coking (review), Appl. Catal. 1983, 5 (3) 263-290.

15. R.V.F. Turcu, A. Samoson, M. Maier, D.L. Trandafir, S. Simon, High fraction of penta-coordinated aluminum and gallium in

lanthanum-aluminum-gallium borates, J. Am. Ceram. Soc. 2016, DOI: 10.1016/j.ceramint.2015.10.004

16. M. Maier, D.L. Trandafir, S. Simon, Effect of heat treatment time on local structure of lanthanum-aluminum-gallium-borate xerogels, Ceram. Int. 2016, 42 (4) 4764-4767.

17. D. Massiot, F. Fayon, M. Kapron, I. King, S. Le Calve, et al., "Modelling One and Two-Dimensional Solid-State NMR Spectra," Magn. Reson. Chem., 40 [1] 70–6 (2002).

18. B. Dou, V. Dupont, P. T. Williams, H. Chen, and Y. Ding, "Thermogravimetric Kinetics of Crude Glycerol,"BioresourceTechnol.,100 [9] 2613–20 (2009).

19. P. Yang, W. Yu, J. Y. Wang, J. Q. Wei, and Y. G. Liu, "LaAl2.03(B4O10) O0.54," Acta Cryst., 54 [1] 11–12 (1998).

20. S. Simon, "Magnetic Resonance Studies on Amorphous and Crystalline Lanthanum Aluminoborates," Phys. Chem. Glasses-B, 47 [4] 489–92 (2006).

21. J. Krogh-Moe, "Interpretation of the Infra-Red Spectra of Boron Oxide and Alkali Borate Glasses," Phys. Chem. Glasses, 6 [2] 46–54 (1965).

22. B. N. Meera and J. Ramakrishna, "Raman Spectral Studies of Borate Glasses," J. Non-Cryst. Solids, 159 [12] 1–21 (1993).

23. S. Simon, R. Grecu, and V. Simon, "Infrared Spectroscopic Studies on Amorphous and Crystalline Lanthanum Aluminoborates," Mod. Phys. Lett. B, 16 [8] 291–8 (2002).

24. T. Satyanarayana, I. V. Kityk, M. Piasecki, P. Bragiel, M. G. Brik, et al., "Structural Investigations on PbO-Sb2O3-B2O3:CoO

Glass Ceramics by Means of Spectroscopic and Dielectric Studies," J. Phys. Condens. Matter., 21 [24] 245104, 16pp (2009).

25. Y. Gandhi, N. Purnachand, K. S. V. Sudhakar, T. Satyanarayana, and N. Veeraiah, "Influence of Modifier Oxides on Some Physical Properties of Antimony Borate Glass System Doped With V2O5," Mater. Chem. Phys., 120 [1] 89–97 (2010).

26. I. N. Chakraborty and D. E. Day, "Effect of R3+ Ions on the Structure and Properties of Lanthanum Borate Glasses," J. Am. Ceram. Soc., 68 [12] 641–5 (1985).

27. A. Jaworski, B. Stevensson, B. Pahari, K. Okhotnikov, and M. Eden, "Local Structures and Al/Si Ordering in Lanthanum Aluminosilicate Glasses Explored by Advanced 27Al NMR Experiments and Molecular Dynamics Simulations," Phys. Chem. Chem. Phys., 14 [45] 15866–78 (2012).

28. A. Masuno, S. Kohara, A. C. Hannon, E. Bychkov, and H. Inoue, "Drastic Connectivity Change in High Refractive Index Lanthanum Niobate Glasses," Chem. Mater., 25 [15] 3056–61 (2013).

29. B. T. Poe, P. F. McMillan, C. A. Angell, and R. K. Sato, "Al and Si Coordination in SiO2-Al2O3 Glasses and Liquids: A Study by NMR and IR Spectroscopy and MD Simulations," Chem. Geol., 96 [34] 333–49 (1992).

30. D.L. Griscom, Borate glass structrure, in: L.D. Pye, V.D. Frechette, N.J. Kreidl (Eds.), Borate Glasses: Structure, Properties, Applications, Plenum Press, New York, 1978, pp. 1–128.

31. L. Fernandez-Carrasco, D. Torrens-Martin, L.M. Morales, S. MartinezRamiez,Infrared spectroscopy in the analysis of building

and construction materials, in: T. Theophanides (Ed.), Infrared Spectroscopy – Materials Science, Engineering and Technology, InTech Europe, Rijeka,2012, pp. 369–382.

32. G. Jagan Mohini, N. Krishnamacharyulu, G. Sahaya Baskaran, N. Veeraiah, Role of Ga2O 3 ions on the structural and bioactive behaviour of B 2O 3–SiO2–P2O5–Na2O–CaO glass system, IJETR 3 (2015) 441–447.

33. W.-H. Huang, C.S. Ray, D.E. Day, Color and selected properties of PbO–BiO1.5–GaO1.5 glasses, J. Am. Ceram. Soc. 77 (1994) 1017–1024.

34. C. Su, D.L. Suarez, Coordination of adsorbed boron: a FTIR spectroscopic study, Environ. Sci. Technol. 29 (1995) 302–311.

35. R.S. Chaliha, A. Tarafder, K. Annapurna, B. Karmakar, Preparation and properties of BaBiBO4–SiO2 glasses, Int. J. Appl. Glass Sci. 1 (2010) 368–377.

36. P. Tarte, Infrared spectra of inorganic aluminates and characteristic vibrational frequencies of AlO4 tetrahedra and AlO6 octahedra, Spectrochim.Acta A 23A (1967) 2127–2143.

37. V.M. Bermudez, S.M. Prokes, Infrared spectroscopy and surface chemistry ofβ-Ga 2O 3 nanoribbons, Langmuir 23 (2007) 12566–12576.

38. D. Tsoutsou, G. Scarel, A. Debernardi, S.C. Capelli, S.N. Volkos, L. Lamagna, S. Schamm, P.E. Coulon, M. Fanciulli, Infrared spectroscopy and X-ray diffraction studies on the crystallographic evolution of La2O 3films upon annealing, Microelectron. Eng. 85 (2008) 2411–2413.

39. T. R. Lopes, G. R. Goncalves, E. de Barcellos Jr, M. A. Schettino Jr, A. G. Cunha, et al., “Solid State 27Al NMR and X-Ray Diffraction Study of Alumina-Carbon Composites,” Carbon, 93, 751–61 (2015).

40. S. Simon, G. J. M. P. van Moorsel, A. P. M. Kentgens, and E. de Boer, “High Fraction of Penta-Coordinated Aluminium in Amorphous and Crystalline Aluminium Borates,” Solid State Nucl. Mag, 5 [2] 163–73 (1995).

41. D. Iuga, S. Simon, E. de Boer, and A. P. M. Kentgens, “A Nuclear Magnetic Resonance Study of Amorphous and Crystalline Lanthanum-Aluminates,” J. Phys. Chem. B, 103 [36] 7591–8 (1999).

42. D. Pan, Q. Xu, Z. Dong, S. Chen, F. Yu, et al., “Facile Synthesis of Highly Ordered Mesoporous Cobalt-Alumina Catalysts and Their Application in Liquid Phase Selective Oxidation of Styrene,”RSCAdv.,5 [119] 98377–90 (2015).

43. S. M. Bradley, R. F. Howe, and R. A. Kydd, “Correlation Between 27Al and 71Ga NMR Chemical Shifts,” Magn. Reson. Chem., 31 [10] 883–6 (1993).

44. D. Massiot, T. Vosegaard, N. Magneron, D. Trumeau, V. Montouillout, et al., “71Ga NMR of Reference GaIV,GaV, and GaVI Compounds by MAS and QPASS, Extension of Gallium/Aluminium NMR Parameter Correlation,” Solid State Nucl. Mag., 15 [3] 159–69 (1999).

45. D. Massiot, R. Revel, C. Magnenet, and D. Bazin, “Characterization of an Al-, Ga-Based Catalyst by Ga NMR and XAS,” Solid State Nucl. Mag., 16 [1–2] 103–8 (2000).

46. F. Turcu, S. Simon, S. Constantinescu, N. Grecu, and D. Iuga, “Structural Changes of Piezoelectric La3Ga5SiO14 Induced by Paramagnetic Ions Revealed by 71Ga Multiple Quantum Magic Angle Spinning,” Solid State Nucl. Mag., 36 [2] 92–5 (2009).

47. A. Caron, B. Doumert, and G. Tricot, “The XGa2O3-(100-x)NaPO3 Glass System: Preparation, Properties and Structural Analysis by Solid State NMR,” Mater. Chem. Phys., 147 [3] 1165–70 (2014).

48. S. B. Narendranath, A. K. Yadav, T. G. Ajithkumar, D. Bhattacharyya, S. N. Jha, et al., “Investigations Into Variations in Local Cationic Environment in Layered Oxide Series in GaO3(ZnO)m (m= 1-4),” Dalton Trans., 43 [5] 2120–6 (2014).

49. I.N. Chakraborty, D.E. Day, Effect of R3+ ions on the structure and properties of lanthanum borate glasses, J. Am Ceram. Soc. 1985, 68 (12) 641–645.

50. M. Maier, D.-L. Trandafir, B. Frentiu, S. Simon, NMR characterization of some lanthanum aluminum gallium borates, Intenational Conference, Bio-Nano-Spec, Cluj-Napoca, Sept. 4-7, 2011.